scientific reports

Check for updates

OPEN

The effect of heteropolyacid-based ionic liquid catalysts for oxidative desulfurization of fuel

Simin Kafash & Amir Abdolmaleki✉

Oxidative desulfurization technology is of interest due to its high efficiency in sulfur removal and mild conditions. The aim of this study is to synthesize a heteropolyacid-based ionic liquids for the removal of benzothiophene compound from model fuel under relatively mild conditions with high efficiency. The catalysts were characterized by FT-IR, ^{1}H-NMR, ^{13}C-NMR, TGA, EDX. Among the studied catalysts, $[CMDMAPy]_3PW_{12}O_{40}$ emerged as the most effective catalyst. With optimized catalyst for the removal of less active BT, using 0.04 g of catalyst, O/S ratio of 8, temperature of 70 °C and 1.5 mL of CH_3CN, removal of 99% of benzothiophene was achieved within 2.5 h. The catalyst exhibits good amphiphilic activity. Which can be attributed to active sites. The reaction results show that the polyoxometalate and carboxylic acid groups have significant effects on the catalytic activity, which can improve the efficiency of ODS. Radical scavenger analysis results indicate that the synergistic effect proceeds from the $O_2^{\bullet-}$ radical pathway. EDX analysis and characterization of the recovered catalyst do not show significant leaching of the catalytic active component.

Keywords Oxidative desulfurization, Brønsted acide, Polyoxometalate, Benzothiophene, Hydrogen peroxide

Recently, the rapid growth of the petrochemical industry has led to increased air pollution from sulfur emissions. Sulfur compounds in fuels, such as mercaptans, thioethers, thiophene, and their derivatives, release harmful sulfur oxides during combustion, contributing to environmental issues such as acid rain and greenhouse gas emissions[1]. As a result, there is a growing demand to control this pollution and reduce the sulfur content of fuels to as low as 10 ppm[2].

Currently, the predominant industrial technique is Hydrodesulfurization (HDS)[3]. HDS is a heterogeneous catalytic process in which sulfur compounds react with hydrogen in the presence of catalysts to produce hydrocarbons and hydrogen sulfide. The HDS process requires severe conditions, such as high temperature and pressure, for efficient sulfur removal. It also involves high catalyst costs and considerable hydrogen usage. While HDS is effective for removing aliphatic sulfur compounds, such as thiols and sulfides, it struggles to remove aromatic sulfur compounds such as thiophene and benzothiophene, which can further increase costs. To overcome these limitations, researchers have explored alternative desulfurization methods, including adsorptive desulfurization (ADS), biodesulfurization (BDS)[4], extractive desulfurization (EDS)[5], and oxidative desulfurization (ODS)[6–8]. Among these, ODS has gained attention because of its ability to effectively remove aromatic compounds under mild conditions.

This method is characterized by high efficiency, low cost, environmental friendliness, and minimal requirements for temperature and pressure, as well as the absence of hydrogen in the ODS; sulfur compounds are first converted to sulfoxides and subsequently to sulfones. Owing to their increased polarity and molecular weight, these compounds can be separated from fuel using an appropriate solvent. The two critical components of ODS are the oxidant and the extractive solvent[9]. Various oxidants have been investigated, with research indicating that hydrogen peroxide (H_2O_2) is particularly effective, yielding sulfones while producing only water as a by-product[10]. Although various solvents and catalysts are employed in this process, a significant challenge in achieving deep desulfurization is the need for highly active catalysis.

The catalysts used in the oxidative desulfurization process can be broadly categorized into two types: homogeneous and heterogeneous. Ionic liquids fall under the category of homogeneous catalysts[11]. Ionic liquids possess several unique properties that have garnered significant attention, including non-flammablility, low vapor pressure, recyclability, and excellent thermal and chemical stability[12]. These characteristics make them ideal candidates for use as green solvents and catalysts.

Numerous studies have demonstrated the effectiveness of various ionic liquids in ODS.

Department of Chemistry, College of Sciences, University of Shiraz, Shiraz 7194684795, Iran. ✉email: abdolmaleki@shirazu.ac.ir

Li et al. demonstrated favorable desulfurization activity by 4-dimethylaminopyridinium-Based, which attributed this good desulfurization performance to the influence of the aromatic π-electron density of the by 4-dimethylaminopyridinium cation. In particular, the results showed that the alkyl chains of the 4-dimethylaminopyridinium cation are beneficial for the desulfurization capacity. The symmetry of the 4-dimethylaminopyridinium ring enhances the π-π interaction between the sulfur atom and the IL. Therefore, sulfur compounds are easily extracted into the IL[13].

One notable advantages of homogeneous catalysts are their uniform distribution within the reaction medium, which enhances the catalytic activity[1415],. Carboxylic acids are among the most commonly employed homogeneous catalysts for the ODS process.

Zhang et al. reported that acidic pyridinium-based cations can exhibit excellent desulfurization performance[16]. Pyridinium compounds are less toxic than other compounds[17].

However, a significant challenge associated with ionic liquids is the difficulty of recovering them and separating the products after the reaction.

Polyoxometalates (POMs) represent a highly versatile class of catalysts for ODS, prized for their structural diversity and multifunctional catalytic properties. For example, EuSbW exhibits excellent catalytic activity in the oxidation of thioethers and alcohols under mild conditions[18], while the hybrid $SiMo_{12}O_{40}$–Cu(2,2′-bipy)$_2$ complex demonstrates both photocatalytic and electrocatalytic performance, highlighting the versatility of POM-based catalysts[19]. Also studies by Prof. Wei Yongge's group demonstrated that amphiphilic hybrid hexavanadates can act as highly efficient emulsion catalysts for deep thiophene oxidation, leveraging water–oil interfacial distribution to accelerate the reaction[20]. Recent studies highlight the broad versatility of POMs in various chemical transformations, including electrocatalytic CO_2 reduction and covalently modified POM-based systems[21,22]. POMs have also been applied in the green synthesis of N-heterocycles, underscoring their broad catalytic versatility[23]. The catalytic efficiency of POMs under mild conditions stems not only from their strong Brønsted and Lewis acidities but also from their distinct redox properties[20,24–26]. For example, polyoxovanadates (POVs), a subfamily of POMs, generate active V-peroxo species in the presence of H_2O_2, which significantly enhance oxidative transformations including the oxidation of sulfur compounds[27]. However, their small specific surface area (less than 10 m^2/g) limits their catalytic activities[28]. To address this limitation, a relatively new approach combines ionic liquids with POMs to enhance the recycling process of homogeneous catalysts while maintaining their effectiveness[29].

The combination of organic cations with heteropolyanions (or polyoxometalate (POM) anions)[30] can lead to the formation of HPA-based ILs salts (ionic-liquid-like structures). Thus, these materials represent a novel class of HPA-based ionic liquids. The presence of organic cations within these salts generates electrostatic interactions between the positively charged cationic ions and negatively charged $[PW_{12}O_{40}]^{3-}$ ions. As a result, $[PW_{12}O_{40}]^{3-}$ ions can be effectively immobilized within the HPA-based ILs salt.

Also In recent years, many other types of POM-IL based on imidazolium and morpholinium have been used as catalysts for oxidative desulfurization[31–34], which can effectively improve the desulfurization efficiency in a short time with the catalyst. While other cations such as 4-dimethylaminopyridinium have been rarely reported, because of the aromatic π-electron density of 4-dimethylaminopyridinium cation, which in addition to its low affinity can have good performance in desulfurization.

There are also few papers on the removal of less active BT from fuel under optimal conditions with high efficiency. Thus, these studies showed that the desulfurization is determined by the cationic groups and the acidity and anion, which affect the interaction between ionic liquids and sulfur compounds.

Finally, in this study, to overcome these shortcomings, we will use 4-dimethylaminopyridinium ionic liquids containing POM to investigate their acidic structure and catalytic performance in the removal of BT from fuel, and we will analyze the effects of different conditions on the effectiveness of this reaction.

Experimental

Materials and methods

N, *N*-Dimethyl aminopyridine-based ionic liquids were synthesized in the laboratory using various reagents and solvents. The materials used in this study were *N*, *N*-dimethyl aminopyridine (DMAP, 99%), bromoacetic acid (98%), bromobutane, phosphotungstic acid ($H_3PW_{12}O_{40}$, 99%), benzothiophene (BT, 99%), hydrogen peroxide(30%), n-heptane (99%), ethanol (99.9%), acetonitrile (99.9%), toluene (99.9%), distilled water, NMR solvents (D_2O, DMSO-d_6, $CDCl_3$), and potassium bromide (KBr). All reagents and solvents were purchased from Merck and Sigma-Aldrich and were used in the preparation of the catalysts and fuel samples without further purification. The catalyst structures and oxidation products were characterized using NMR spectroscopy on a 400 MHz Avance DPX Bruker spectrometer with $CDCl_3$, D_2O, and DMSO-d_6 as solvents. FT-IR spectra were obtained with a Bruker Vector 22 FT-IR spectrophotometer in the solid-state using KBr, covering the range of 400–4000 cm^{-1}. Thermogravimetric analysis (TGA) of the samples was performed using a Linseis L81 instrument under a nitrogen atmosphere. Contact angles (CAs) were evaluated using a U-VISION MV500 camera (China) by analyzing a water droplet and n-heptane. Ultraviolet-visible (UV-Vis) spectra were obtained with a PerkinElmer LAMBDA 365 spectrometer. The elemental analysis of the catalysts was conducted using an energy-dispersive X-ray (EDX) spectroscopy system connected to a Philips scanning electron microscope (SEM). The sulfur content of gasoline was measured using the multi EA 5000 analyzer manufactured by Analytik Jena, with the assistance of the Persian Golf Star Oil Company. Gas chromatography (GC-MC) analyses were conducted on an Agilent 7890B system equipped with a BPX5 capillary column (30 m × 0.25 mm i.d. × 0.25 µm).

Preparation of the catalysts

The route of synthesis for catalyst $[CMDMAPy]_3PW_{12}O_{40}$ following established literature methods[35] was synthesized in two steps is outlined in Fig. 1. In the first step, 50 mmol of bromoacetic acid was dissolved in 3 mL

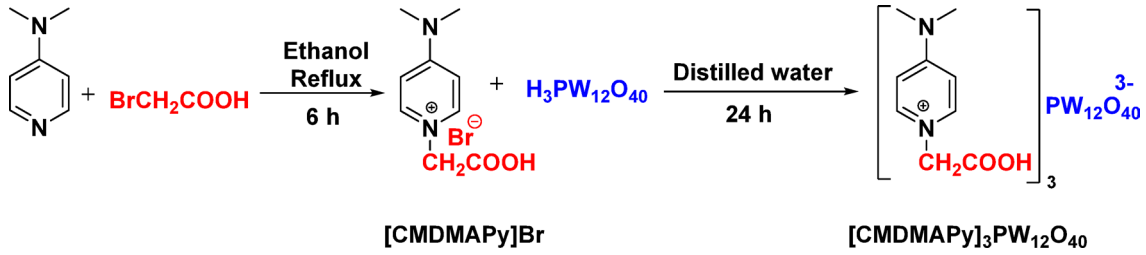

Fig. 1. Schematic illustration step for preparation of POM-IL.

of ethanol in a 50 mL round bottom flask, which was then placed in an ice bath. Over 1.5 h, DMAP (50 mmol) dissolved in ethanol (5 mL) was added dropwise to the flask. Subsequently the reaction mixture was refluxed in an oil bath for 6 h, resulting in the formation of a precipitate. The precipitate was then washed with cold ethanol and dried at room temperature. In the second step, according to the literature[36], the ionic liquid was reacted with phosphotungstic acid at a 3:1 molar ratio. A solution of the synthesized ionic liquid (3 mmol) in distilled water was added dropwise to a solution of phosphotungstic acid (1 mmol) at room temperature. The precipitate formed was washed with distilled water and vacuum-dried for 24 h. $(C_4DMAP)_3PW_{12}O_{40}$ were prepared based on the same method using the corresponding starting materials. The structure of the final product was confirmed using FT-IR, ^{1}H-NMR and^{13}C-NMR spectroscopy.

[CMDMAPy]$_3$ $PW_{12}O_{40}$ was obtained as Yellow solid. ^{1}H-NMR (DMSO-d_6, 400 MHz): δ = 3.22 (s, 6 H), δ = 5.05 (s, 2 H), δ = 7.05–7.07 (d, 2 H), δ = 8.20–8.22 (d, 2 H). ^{13}C-NMR (DMSO-d_6, 100 MHz): δ = 39.52, 57.25, 107.74, 143.54, 156.44, 169.44 ppm. IR (KBr, cm^{-1}): 807 (W-O_c-W), 895 (W-O_b-W), 977 (W = O_t), 1079 (P-O_a), 1176 (C-N), 1652 (C = N), 1735 (C = O), 2936 (C–H), 3095 (C–H), 3540 (O–H). Elemental analysis ([CMDMAPy]$_3$ $PW_{12}O_{40}$): C (9.95%), N (3.51%), O (13.01%), P (1.29%), W (72.25%).

[C_4DMAPy]$_3$ $PW_{12}O_{40}$ was obtained as Yellow solid. ^{1}H-NMR (DMSO-d_6, 400 MHz): δ = 0.88–0.92 (t, 3 H), δ = 1.20–1.29 (m, 2 H), δ = 1.71–1.78 (m, 2 H), δ = 3.19 (s, 6 H), δ = 4.14–4.18 (t, 2 H), δ = 7.02–7.04 (d, 2 H), δ = 8.29–8.31 (d, 2 H). ^{13}C-NMR (DMSO-d_6, 100 MHz): δ = 13.84, 19.21, 32.77, 40.58, 56.93, 108.13, 142.42, 156.27 ppm. IR (KBr, cm^{-1}): 799 (W-O_c-W), 894 (W-O_b-W), 977 (W = O_t), 1079 (P-O_a), 1176 (C-N), 1652 (C = N), 2932 (C–H), 3087 (C–H), 3515 (O–H). Elemental analysis ([C_4DMAPy]$_3$ $PW_{12}O_{40}$): C (10.91%), N (2.95%), O (9.81%), P (1.54%), W (74.79%).

[CMDMAPy] Br was obtained as white solid. ^{1}H-NMR (DMSO-d_6, 400 MHz): δ = 0.88–0.92 (t, 3 H), δ = 1.20–1.29 (m, 2 H), δ = 1.71–1.78 (m, 2 H), δ = 3.19 (s, 6 H), δ = 4.14–4.18 (t, 2 H), δ = 7.02–7.04 (d, 2 H), δ = 8.29–8.31 (d, 2 H). ^{13}C-NMR (DMSO-d_6, 100 MHz): δ = 13.84, 19.21, 32.77, 40.58, 56.93, 108.13, 142.42, 156.27 ppm. IR (KBr, cm^{-1}): 1176 (C-N), 1652 (C = N), 1740 (C = O), 2935 (C–H), 3068 (C–H), 3444 (O–H). Elemental analysis ([CMDMAPy] Br): C (44.74%), N (18%), O (7.85%), Br (29.92%).

[C_4DMAPy] Br was obtained as white solid. ^{1}H-NMR (D_2O, 400 MHz): δ = 0.76–0.80 (t, 3 H), δ = 1.12–1.22 (m, 2 H), δ = 1.66–1.73 (m, 2 H), δ = 3.06 (s, 6 H), δ = 3.97–4.01 (t, 2 H), δ = 6.72–6.75 (d, 2 H), δ = 7.86–7.89 (d, 2 H). ^{13}C-NMR (D_2O, 100 MHz): δ = 12.64, 18.63, 31.97, 39.25, 57.38, 107.40, 141.25, 156.25 ppm. IR (KBr, cm^{-1}): 1176 (C-N), 1652 (C = N), 2951 (C–H), 3031 (C–H). Elemental analysis ([C_4DMAPy] Br): C (54.96%), N (20.87%), Br (24.17%).

Oxidation desulfurization of the model fuel process

The model fuel was prepared with a sulfur content of 500 ppm, consisting of benzothiophene (BT) dissolved in n-heptane. The oxidation of sulfur (ODS) was performed in a 50 mL glass flask. The flask was charged with 30% H_2O_2, acetonitrile, model fuel and catalyst. The reaction proceeded for 2.5 h under stirring and heating at 70 °C. After the reaction was complete, the mixture was cooled to room temperature, resulting in separation of the two phases. The polar solvent settled at the bottom of the flask, whereas the unreacted oil phase remained at the top. The oil phase was analyzed directly by gas chromatography using an Agilent 7890B equipped with a BPX5 capillary column (30 m × 0.25 mm i.d. × 0.25 μm). The extent of sulfur removal was calculated using the following equation:

$$S(\%) = [(C_0 - C_t)/C_0] \times 100\% \quad (1)$$

C_0 represents the initial concentration of sulfur in the model fuel, and C_t is the concentration of sulfur in the model oil after desulfurization.

Results and discussion

Characterization of the catalysts.

The results of the interaction between the heteropolyacid anions and IL cations were analyzed using the IR spectrum presented in Figure S 1 For [C_4DMAPy]$_3$$PW_{12}O_{40}$ and [CMDMAPy]$_3$$PW_{12}O_{40}$, the peaks at 1097, 977, 895, and 807 cm^{-1}, were attributed to the stretching frequencies of P-O_a, W = O_t, W-O_b-W and W-O_c-W, respectively[37]. These finding are consistent with the phosphotungstic acid spectrum. Additionally, C = C stretching bands, along with aliphatic C-H and aromatic C-H stretching bands typical of the pyridinium cation, were observed at 1569, 2935 and 3068 cm^{-1} in all structures. To further confirm the presence of the pyridinium cation, C-N and C = N stretching bands were identified at 1176 and 1652 cm^{-1}. In Figure S 1 (C), the broad peak

at 3444 cm^{-1} corresponds to the OH functional group, while the peak at 1740 cm^{-1} is associated with the acidic carbonyl group indicating the catalytic structure of [CMDMAPy]Br. Overall, the IR spectra were consistent with the structure depicted in Fig. 1. The ^{1}H-NMR and ^{13}C-NMR characterization results further confirmed the chemical structure of the four HPA-IL salts.

The synthesized catalysts containing bromines anion and heteropolyacids were characterized using ^{1}H-NMR and ^{13}C-NMR in D_2O and DMSO-d_6 (Fig. S2-S9). The NMR spectra of the ionic liquids align with the desired structures depicted in Fig. 1, confirming the successful synthesis of the catalysts and the high purity of the obtained ionic liquids. The presence of nitrogen within the ring, which carries a positive charge, along with acidic groups that act as electron-withdrawing groups, results in the deshielding of hydrogen atoms. Additionally, the hydrogen peak of carboxylic acid was absent in the NMR spectra due to proton exchange with D_2O and DMSO-d_6. For further confirmation, the peak appearing at ^{13}C-NMR at 170 confirmed the presence of acidic groups.

In this study, thermogravimetric analysis was conducted in a N_2 atmosphere to assess the thermal stability of pure catalysts (ionic liquid) and those derived from heteropolyacid. As anticipated, the ionic liquid (IL) hybrids exhibited significant weight reduction compared to their corresponding heteropolyacids[38]. Figure S 10., shows that the decomposition temperatures of the [C_4DMAPy]Br and [CMDMAPy]Br catalysts are approximately 240 °C, with a mass reduction of 90.48% and 75.64%. At higher temperatures, from 220 °C to 350 °C is the destruction of the main carbon structure leads to a substantial decrease in stability. In contrast, the weight analysis of the [C_4DMAPy]$_3PW_{12}O_{40}$ and [CMDMAPy]$_3$ $PW_{12}O_{40}$ catalysts revealed higher decomposition temperatures, indicating enhanced thermal stability. Notably, the presence of phosphotungstic acid has varying effects on the thermal stability within the temperature range of 300–400 °C. In this range, phosphotungstic acid slightly improved the thermal stability of [C4DMAPy]$_3$ $PW_{12}O_{40}$ and [CMDMAPy]$_3$ $PW_{12}O_{40}$ compared to that of [C_4DMAPy]Br and [CMDMAPy]Br. The major weight loss 1.94% and 7.8% from 320 °C to 500 °C is presumably caused by the decomposition of the loaded ILs. The weight loss that occurs after about 500 °C may be due to the decomposition of the polyoxometalate anion structure[39]. Similar observations have been reported, which showed thermal stability up to 300 °C, supporting the inherent robustness of POM-based systems[40].

EDX spectroscopy confirms the accumulation of C, N, O, W and P elements in the synthesized catalyst. The weight% (wt%) of these elements is 9.95, 3.51, 13.01, 1.29, 72.25%, respectively (Fig. S 13). Also, the elemental mapping results show that all the mentioned elements are uniformly distributed on the catalyst surface. EDX mapping also confirms the elemental percentages for other catalysts (Fig. S 11, 12 and 14).

Contact angle test was performed to determine the wettability of the catalyst by water and heptane. The contact angle was Θ= 5.18° when a drop of water was dropped on the catalyst surface (Fig. S 15, A) and when tested with heptane the contact angle was almost Θ= 0° (Fig. S 15, B), indicating the high wettability of the catalyst.

Desulfurization with different catalysts

Benzothiophene is one of the aromatic compounds present in fuels, and few studies have specifically addressed the high removal of this compound from fuels, which was not sufficient. For a better understanding of the correlation between catalyst and desulfurization efficiency, the BT desulfurization done under different systems.

We used benzothiophene to oxidize sulfur compounds in model fuels by [CMDMAPy] $_3PW_{12}O_{40}$ to optimize the reaction conditions. In our initial experiments, the extractive desulfurization reaction without oxidant had about 30% sulfur removal, which was a low removal efficiency (Table 1, entry 1). To improve the removal conditions, hydrogen peroxide was used as the oxidant in oxidative desulfurization, but in the absence of a catalyst, only 5.5% sulfur removal occurred, which was a very low efficiency (Table 1, entry 2).

(Table 1, entries 3 and 4) highlight the important role of the acid group. When a catalyst with carboxylic acid groups is used, sulfur removal increases by 51%. These results indicate that ionic liquids with carboxylic acid groups contribute to desulfurization. In the presence of hydrogen peroxide, the acid group was converted to the active form of peroxycarboxylic acid, facilitating rapid sulfur removal, but the benzothiophene removal was still low, while in the presence of phosphotungstic acid, sulfur removal was improved by up to 99% (Table 1, entries 5 and 6), which shows that in addition to the type of ionic liquid, the phosphotungstic acid group also plays an important role in the reaction and acts as the catalytically active component. After reaction with hydrogen peroxide, the phosphotungstic acid-modified catalysts produce active peroxy species that convert benzothiophene to sulfone compounds. These results indicate that due to the synergistic effect of POM and ILs

Entry	Catalysts	BT removal (%)
1	[CMDMAPy]$_3$ $PW_{12}O_{40}$ [a]	30
2	H_2O_2 [b]	5.5
3	[C_4DMAPy]Br	35.1
4	[CMDMAPy]Br	51.5
5	[C_4DMAPy]$_3$ $PW_{12}O_{40}$	83.4
6	[CMDMAPy]$_3$ $PW_{12}O_{40}$	99

Table 1. Effect of desulfurization systems on BT Removal. Reaction conditions: Fuel = 10 mL, m (catalyst) = 0.04 g, temperature = 70 °C, time = 2.5 h, O/S = 8, 1.5 mL MeCN. [a]Reaction conditions: Fuel = 10 mL, m (catalyst) = 0.04 g, temperature = 70 °C, time = 2.5 h, 1.5 mL MeCN. [b]Reaction conditions: Fuel = 10 mL, temperature, time = 2.5 h, O/S = 8, 1.5 mL MeCN.

containing carboxylic acid groups, they are important for BT oxidation in the ODS system. Similar to previous reports showing that the rigid structure and exposed active sites of $[W_{10}O_{32}]^{4-}$ enhance reactivity in C–H functionalization[41], the high desulfurization efficiency of $[CMDMAPy]_3PW_{12}O_{40}$ can be attributed to the dual active sites provided by the POM and ionic liquid framework, which synergistically promote BT oxidation. Among the synthesized catalysts, $[CMDMAPy]_3PW_{12}O_{40}$ exhibited the highest desulfurization efficiency, highlighting the importance of these dual active sites.

Effect of acidity of HPA-ILs salts on desulfurization efficiency

The Hemmett relationship was used to evaluate the acid strength. This method is suitable for investigating the protonation tendency in environments containing ionic compounds and can be performed using a protonatable indicator. In this study, the UV-vis spectroscopy technique was used based on previous studies[32]. This method is based on determining the concentration ratio of protonated and unprotonated indicator species [I]/[IH+] in the solution. UV-VIS spectra show that this marker absorbs at a wavelength of 378 nm in dimethyl sulfoxide. Using this equation,

$$H_0 = pK(I)aq + \log([I]/[IH+]) \quad (2)$$

the H0 value (acid strength index) can be calculated.

In this study, the indicator 4-nitroaniline (4 mmol/L) and (which has a pK(I) = 0.99) were prepared. A solution (4 mmol/L) of ionic liquids was prepared and after adding a certain amount of the desired solution to the solution containing the indicator, its absorption spectrum was recorded by a UV-vis spectroscopy. The [I]/[IH+] ratio was calculated from the spectral data and, accordingly, the H0 values were determined for different compounds.

The results are shown in Table S1, according to the UV-vis data in Figure S16, the order of acidity is as follows: $[CMDMAPy]_3PW_{12}O_{40}$ > $[C_4DMAPy]_3PW_{12}O_{40}$ > [CMDMAPy]Br > $[C_4DMAPy]$Br.

In the oxidative desulfurization experiments according to Table 1, $[CMDMAPy]_3PW_{12}O_{40}$ had higher desulfurization efficiency than other catalysts, indicating that when the acidity increases, the desulfurization efficiency also increases.

Effects of different factors on the sulfur removal of BT

The effect of catalyst quantity on sulfur removal in a 10 mL model fuel was investigated. As illustrated in Fig. 2a, a direct relationship between the catalyst dosage and desulfurization efficiency was observed; desulfurization increased progressively as the catalyst dosage increased. The results showed that the desulfurization efficiency reached 99%, after 2.5 h of reaction. As the catalyst dosage increased, the available surface area also increased, thus providing more active sites for the binding of sulfur components. Desulfurization reached its maximum when the dosage was increased from 0.01 to 0.04 g. However, when the catalyst dosage beyond 0.04 g, the desulfurization efficiency decreased. This implied that there were enough active sites for the oxidation of sulfur

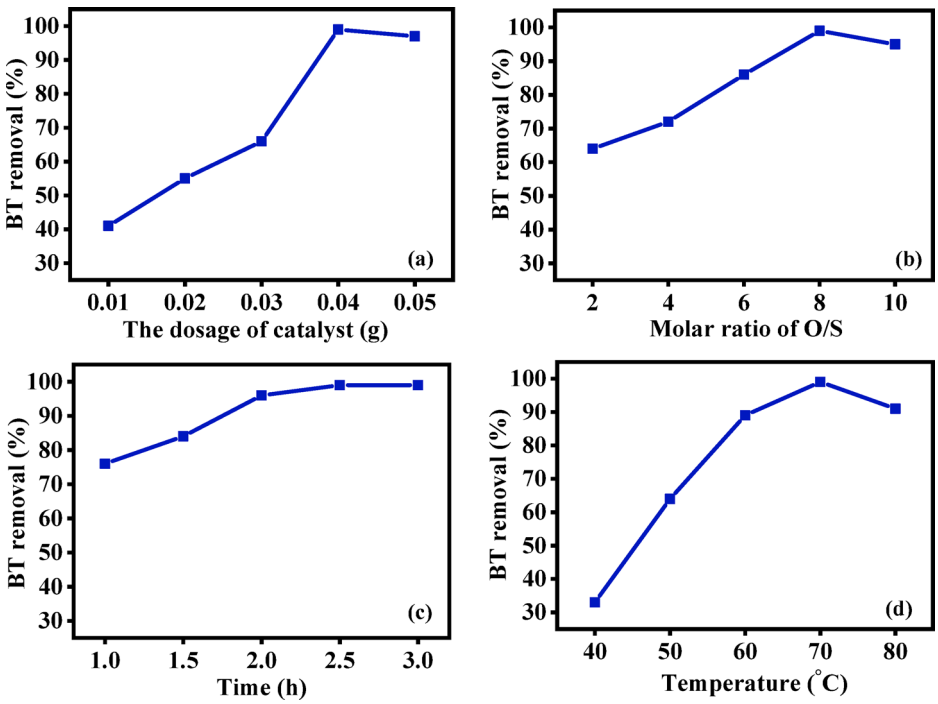

Fig. 2. Effect on the desulfurization rate of benzothiophene (BT) removal: (**a**) catalyst of dosage, (**b**) molar ratio of O/S, (**c**) reaction time and (**d**) reaction temperature..

compounds in the case of 0.04 g catalyst's dosage. However, if the amount exceeds 0.04 g, excessive accumulation can hinder the absorption of benzothiophene, thereby limiting the overall effectiveness[33]. Therefore, 0.04 g of catalyst was chosen as the suitable amount in the experiment.

Hydrogen peroxide (30%) was used as the oxidant in the desulfurization reaction. To investigate the influence of the amount of oxidant, BT was first oxidized at various O/S molar ratios. As shown in Fig. 2b, the O/S molar ratio significantly affected BT removal. As the amount of oxidant increased, the desulfurization rate also increased. The BT removal increased from 65% at O/S = 2 to 86% at O/S = 6 in 2.5 h when O/S = 8, and BT removal reached 99% in 2.5 h. However, excessive hydrogen peroxide consumption led to the production of more water, which diluted acetonitrile and hindered benzothiophene extraction. Consequently, when the O/S ratio exceeded 8, benzothiophene removal decreased. Therefore, it is essential to maintain a sufficient oxidant concentration to achieve an optimal desulfurization efficiency. Therefore, the O/S molar ratio of 8 was chosen as the optimal ratio.

To evaluate the effect of time on the extraction efficiency, the extraction of model fuel using $[CMDMAPy]_3PW_{12}O_{40}$ was performed over various durations: 1, 1.5, 2, 2.5, and 3 h. As the reaction time increased, the desulfurization efficiency increased rapidly, reaching a maximum after 2.5 h, Fig. 2c. However, the S-concentration continuously decreased with increasing extraction time. When the reaction proceeded to a certain extent, a small amount of BT existed in the model fuel phase, so that the extraction rate decreased and BT removal was no longer marked. Thus, the optimal reaction time for this catalyst is determined to be 2.5 h.

The effect of temperature on BT removal is shown in Fig. 2d. The results clearly show that desulfurization increased continuously with increasing reaction time. At 40 °C, the sulfur removal rate after 2.5 h was 28%, whereas at 70 °C, it increased to 99%, highlighting the significant effect of temperature on desulfurization. During this period, the concentration of the active species responsible for sulfur removal increased. The quantity of the peroxometal complex formed increased with temperature, and its oxidative ability toward BT was enhanced. However, no considerable effect was observed with a further increase in temperature. Increasing the temperature to 80 °C decreased the absorption of benzothiophene. This decline can be attributed to the decomposition of the oxidant, which reduces the availability of the peroxycomplex and peroxycarboxylic acid species, ultimately lowering the sulfur removal efficiency. Additionally, the elevated temperature causes the heptane solvent in the fuel to reach its boiling point, further diminishing the effectiveness of sulfur removal.

Effect of the acetonitrile amount on desulfurization

The choice of solvent can significantly affect the efficiency of sulfur removal. Polar solvents tend to interact more favorably with polar sulfur compounds, enhancing their solubility. Figure 3, shows that acetonitrile significantly influenced the benzothiophene extraction process. When the desulfurization test was conducted without acetonitrile as the extractant, the removal rate of BT in the model fuel reached 52% for $[CMDMAPy]_3PW_{12}O_{40}$, which was the result of the combination of oxidant and catalyst. With an increase in the extractant dosage, the desulfurization effect significantly improved. The acetonitrile solvent forms a two-phase system by dissolving the heteropolyacid catalyst, facilitating the transfer of benzothiophene into the polar phase and enabling its rapid removal. When the amount of extractant was greater than 1.5 mL, the desulfurization efficiency improved slightly. Therefore, 1.5 mL of extractant was suitable for BT extraction.

Effect of sulfur content on BT removal

BT removal in the model fuel was investigated at different sulfur concentrations (100, 250, 500, and 1000 ppm). Figure 4 shows that the BT removal for the model fuel of less than 1000 ppm reached 99% in 2.5 h. However, when the BT content was increased to 1000 ppm, BT removal decreased to 77.58%. These results indicate a decrease in the efficiency of the ODS system for samples with high sulfur content.

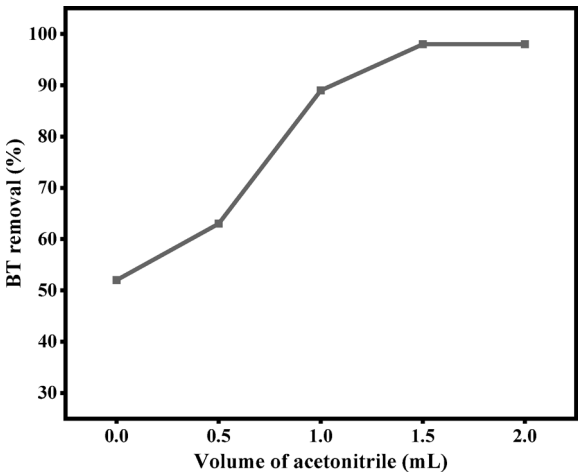

Fig. 3. Effect of the acetonitrile amount on the conversion of the BT. Reaction conditions: initial sulfur content 500 ppm, 10 mL of model fuel, O/S = 8, cat (0.04 g), 70 °C, 2.5 h..

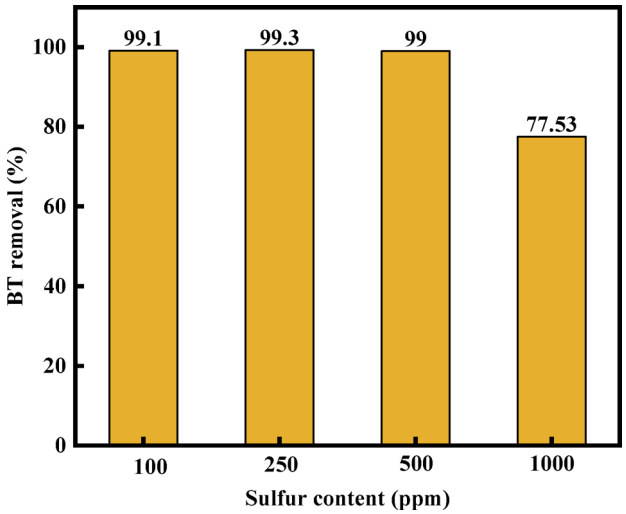

Fig. 4. Effect of Sulfur concentration on BT removal. Reaction conditions: 10 mL of model fuel, O/S = 8, cat. 0.04 g, 70 °C, 2.5 h, 1.5 mL MeCN.

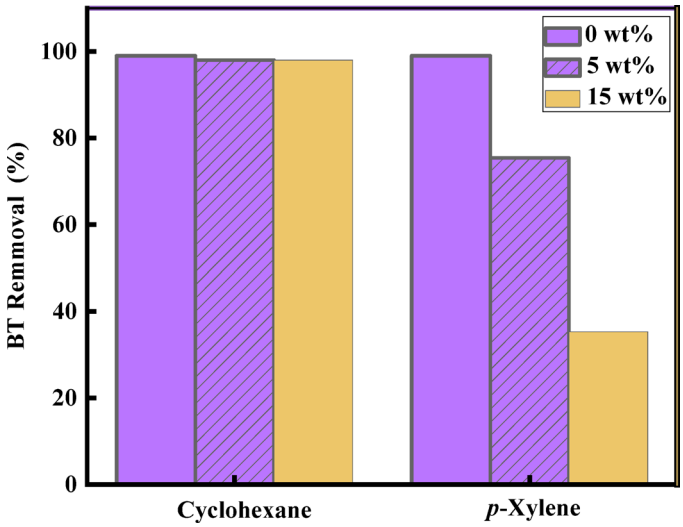

Fig. 5. Effect of cyclohexane/*p*-xylene on desulfurization efficiency (O/S = 8, cat. 0.04, 70 °C, 2.5 h, 1.5 mL MeCN).

Effect of other components on BT removal

Given the complexity of the structure of fuel compounds, it is necessary to investigate the effect of additives on the desulfurization process in more detail. In this regard, it is necessary to investigate the effect of additives on the desulfurization process in more detail. In this regard, cyclohexane and p-xylene compounds were used in weight percentages of 5% and 15% and their effect on benzothiophene removal was evaluated. The results from (Fig. 5) show that cyclohexane had the same effect at both concentrations and the removal efficiency was very high, but the use of p-xylene at a concentration of 5% reduced the BT removal efficiency to 75.38% and with an increase in the concentration to 15%, the efficiency decreased to 45.3%. Therefore, p-xylene has an inhibitory effect in the desulfurization system.

Effect of the recycle of the catalysts

The recovery process of ionic liquids and catalysts for industrial applications is crucial because it can help reduce costs and enhance efficiency. After the reaction, distillation was performed to remove water and hydrogen peroxide from the sulfone-containing catalyst. The catalyst was washed with chloroform, allowing separation of the sulfone product and regeneration of the catalyst. After distillation, chloroform phase containing a yellow crystalline precipitate was formed. The catalyst demonstrated excellent recyclability, maintaining approximately 91% sulfur removal efficiency over six reuse cycles, without a significant decline in performance Fig. 6a. This indicates the high stability of the catalyst even after multiple uses. The observed decrease in BT removal may be

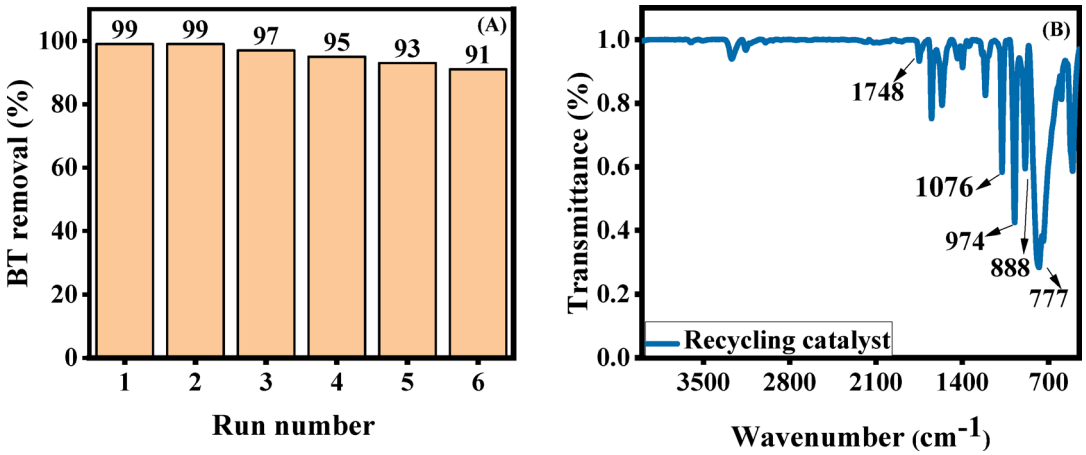

Fig. 6. Effect of $[CMDMAPy]_3PW_{12}O_{40}$ recycling on ODS of model oil (a), FT-IR pattern of reused catalyst (b).

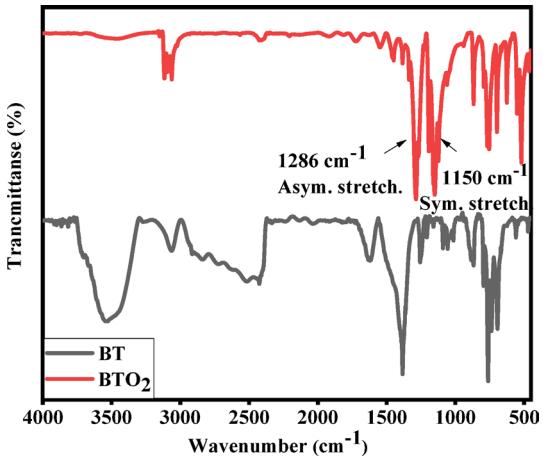

Fig. 7. FT-IR spectra of BT and its oxidation product.

attributed to the retention of BTO2 in the layer, which persist even after several extraction steps using chloroform. Figure 6b shows the FT-IR spectra after the catalyst was reused. The characteristic stretching vibration and diffraction peaks of phosphotungstic acid clearly show that the active components of the catalyst were able to maintain their original structure without any major degradation or changes. This is because the catalyst maintained good catalytic performance during the recycling experiment. ^{1}H-NMR and ^{13}C-NMR analysis (Fig. S 21- S 22) of the recovered catalyst confirmed that the original structure remained somewhat intact after several washing cycles.

The structure of the sulfone was confirmed using FT-IR[42], ^{1}H-NMR, ^{13}C-NMR and GC-MS[43]. In the IR analysis Fig. 7, the appearance of two peaks at frequencies of 1150 and 1286 cm^{-1} corresponded to the functional group representing S = O, which was formed during the oxidation of benzothiophene to the sulfone product BTO_2. To further investigate the process of the ODS system, GC-MS analysis of the catalyst phase was performed to identify the BT product after the reaction; the results are shown in Fig. 8. As can be seen, the peak at about 32 min was attributed to BT sulfone (BTO_2, m/z = 166.0), and no other products were detected in the oxidation phase. Additional information regarding the 1H-NMR and[13]C-NMR spectra of BT and BTO_2 is provided in (Fig. S 17– S 20).

Real diesel desulfurization

In this study, the effect of using real fuel instead of model fuel was investigated. The initial sulfur of the fuel was measured by a total sulfur device and the initial sulfur concentration was recorded as 53.86 ppm. In this experiment, $[CMDMAPy]_3PW_{12}O_{40}$ was used as the catalyst and under the optimal conditions of 10 mL of model fuel, O/S = 8, cat. 0.04 g, 70 °C, 2.5 h, 1.5 mL MeCN. The results show that the presence of more complex compounds in the real fuel can affect the catalyst performance and the overall efficiency of the process. However, the system used was able to decrease the sulfur content to 32.26 ppm, which is equivalent to 40% sulfur removal. These results indicate that the catalyst has the potential to be used in industrial applications.

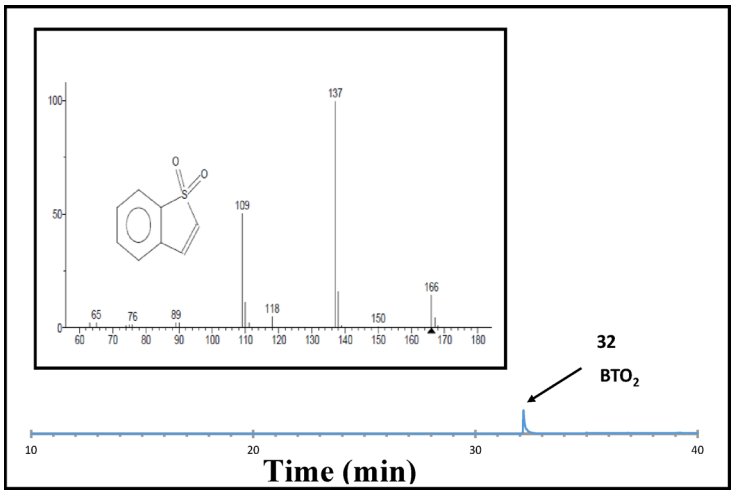

Fig. 8. GC–MS analysis of catalyst phase extracted with chloroform.

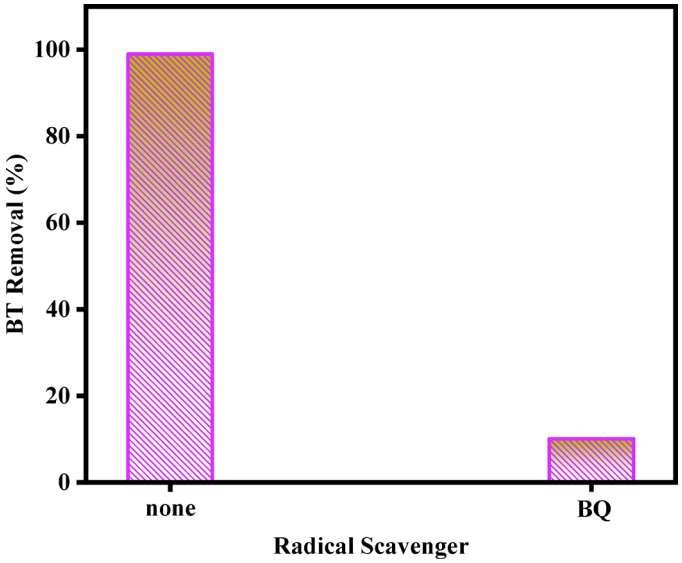

Fig. 9. The free radical scavenger using BQ mechanism for the desulfurization process of BT with $[CMDMAPy]_3\ PW_{12}O_{40}$ (O/S = 8, cat. 0.04, 70 °C, 2.5 h, 1.5 mL MeCN).

Mechanism of ODS process

Previous studies have also demonstrated that the COOH group can be converted into peroxycarboxylic acid in the presence of hydrogen peroxide[16]. Additionally, catalysts based on heteropolyacid groups can generate active peroxide species in the hydrogen peroxide is present[32]. Table 1 indicates that acid catalysts outperform neutral catalysts in desulfurization efficiency, highlighting the essential roles of the COOH and phosphotungstic acid groups within the structure of ionic liquids, which enhance desulfurization effectiveness. Various radical scavengers are used to capture radicals produced in the reaction process. In this system, benzoquinone (BQ) was used to investigate the active species. The desulfurization results show that in the absence of BQ, the desulfurization activity did not change, but in the presence of BQ, a decrease in desulfurization activity was observed Fig. 9. This observation indicates that BQ plays a key role in trapping free radicals and confirms the presence of $HO^{\bullet}$ and $O^{2\bullet-}$ radical species in the system[44]. Similar findings have been reported in other POM-based photocatalytic systems, where reactive oxygen species, especially $O_2\bullet-$, were shown to be involved in the reaction pathways, supporting the proposed mechanism in this work[45]. The symmetry of the 4-dimethylaminopyridinium ring enhances the π-π interaction between the sulfur atom and the IL. Therefore, sulfur compounds are easily extracted into the IL[13]. Furthermore, selection of an appropriate polar solvent can create an optimal reaction environment. The $[CMDMAPy]_3PW_{12}O_{40}$ catalyst, when combined with acetonitrile, plays a multifunctional role in the oxidative desulfurization system. Figure 10, illustrates that the oxidation process begins with the extraction of benzothiophene from the oil phase into the polar phase facilitated by acetonitrile. Initially, the oxygen from the phosphotungstic acid anion (WO) is oxidized to tungsten peroxide ($W(O_2)$) in the presence

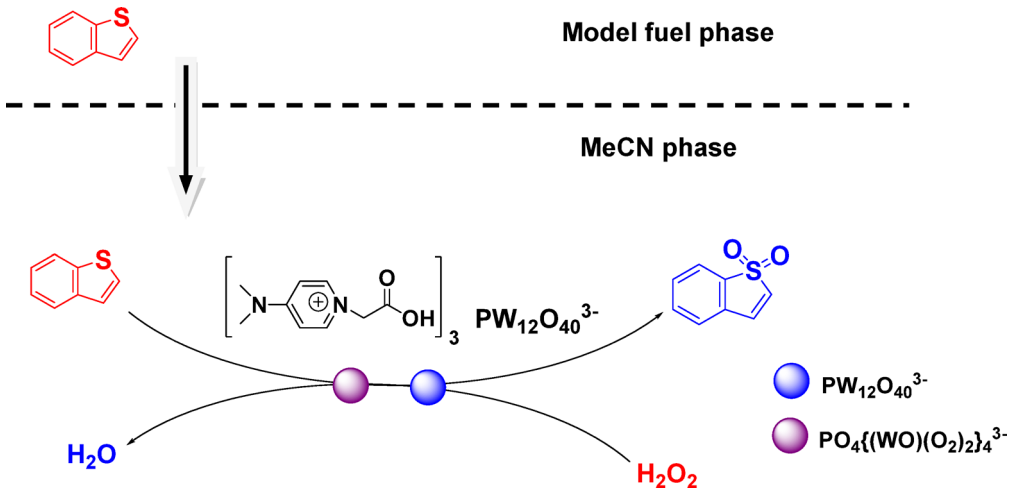

Fig. 10. Process of extraction and oxidation reaction of BT in an fuel-HPA-ILs.

Catalyst	Catalyst (g)	Temp. (°C)	Time (h)	$n(H_2O_2)/n(S)$	S-Removal (%)	Ref
$[C_2(MIM)_2]PW_{12}O_{40}$	0.025	50	1	6	98.0	[34]
$[C_4ImBS]_3[PW_{12}O_{40}]$	0.02	60	2	6	100	[31]
$C_{12}PW/g\text{-}C_3N_4$	0.05	60	1	4	100	[46]
$[C_3SO_3Hnhm]_3PW_{12}O_4$	0.02	50	1.75	15	99.4	[32]
$[CMDMAPy]_3PW_{12}O_4$	0.04	70	2.5	8	99.0	This work

Table 2. Comparison of different catalysts for removal of model fuel.

of hydrogen peroxide. The sulfur atom in BT was then converted to sulfone through the action of tungsten peroxide, which was subsequently reduced to its original state. As the reaction progressed, the polarity of the sulfur bond increased, making its extraction by the solvent easier. At the end of the reaction, the sulfur-free fuel could be separated from the surface, while the sulfone could be removed. The catalyst was then extracted using chloroform, which allowed its reuse.

A short review of comparisons with previous work

Table 2 shows a comparison of the benzothiophene removal efficiency of $[CMDMAPy]_3PW_{12}O_{40}$ prepared in this study with those of other published works. In previous reports, the desulfurization efficiency was for the removal of dibenzothiophene, the efficiency obtained in this work was for the removal of benzothiophene. Because benzothiophene is slightly more difficult to oxidize than other sulfur compounds, we were able to obtain excellent performance for the removal of benzothiophene using the $[CMDMAPy]_3PW_{12}O_{40}$ catalyst within a reaction time of 2.5 h, indicating its potential as an efficient and promising catalyst for the ODS reaction.

Conclusion

In conclusion, COOH-functionalized POM-based IL catalysts were easily and successfully synthesized using a two-step method, and their structures were characterized by IR, NMR, and TGA. The performance of the catalysts in the desulfurization of fuel containing benzothiophene was evaluated using hydrogen peroxide, and a remarkable sulfur removal efficiency of 99% was achieved. Key factors influencing the oxidation reaction during benzothiophene desulfurization include the presence of the COOH group and heteropolyacid, which form an active peroxide group, thereby enhancing the oxidation activity. Additionally, the use of acetonitrile facilitated the extraction of benzothiophene into the polar phase, further improving desulfurization efficiency. The catalyst $[CMDMAPy]_3PW_{12}O_{40}$ demonstrated optimal performance under the following reaction conditions: initial sulfur content 500 ppm, 10 mL model oil, O/S ratio of 8, catalyst amount of 0.04 g, temperature of 70 °C, and a reaction time of 2.5 h. It exhibited high stability and could be recycled up to six times with only a slight decrease in desulfurization efficiency.

Although this study employed model fuels, optimizing POM-IL catalysts for benzothiophene removal provides a critical foundation for treating complex real-world fuels containing diverse sulfur species.

Data availability

All data generated or analyzed during this study are included in this published article (and its supplementary information file).

Received: 12 February 2025; Accepted: 29 September 2025
Published online: 04 November 2025

References

1. Panwar, N. L., Kaushik, S. C. & Kothari, S. Role of renewable energy sources in environmental protection: A review. *Renew. Sustain. Energy Rev.* **15**, 1513–1524 (2011).
2. Kumar, S. et al. An eco-friendly cryogenic fuel for sustainable development. *Appl. Energy*. **88**, 4264–4273 (2011).
3. Calin, C. et al. Mutual Inhibition effect of sulfur compounds in the hydrodesulfurization of thiophene, 2-ethylthiophene and benzothiophene ternary mixture. *Sci. Rep.* **11**, 19053 (2021).
4. Chen, S. et al. Efficient biodesulfurization of diesel oil by Gordonia sp. SC-10 with highly hydrophobic cell surfaces. *Biochem. Eng. J.* **174**, 108094 (2021).
5. Abro, R. et al. Extractive desulfurization of fuel oils using deep eutectic solvents – A comprehensive review. *J. Environ. Chem. Eng.* **10**, 107369 (2022).
6. Vedachalam, S. & Dalai, A. K. Hydrotreating and oxidative desulfurization of heavy fuel oil into low sulfur marine fuel over dual function NiMo/γ–Al2O3 catalyst. *Catal. Today*. **407**, 165–171 (2023).
7. Wu, P. et al. Understanding oxygen doping effects on Boron nitride catalysis for efficient oxidative desulfurization of fuel oil. *Appl. Catal. B Environ. Energy*. **347**, 123784 (2024).
8. Wu, P. et al. Few-layered hexagonal Boron nitride nanosheets stabilized Pt NPs for oxidation promoted adsorptive desulfurization of fuel oil. *Green. Energy Environ.* **9**, 495–506 (2024).
9. Zhang, J., Wang, A., Li, X. & Ma, X. Oxidative desulfurization of Dibenzothiophene and diesel over [Bmim]3PMo12O40. *J. Catal.* **279**, 269–275 (2011).
10. Zapata, B., Pedraza, F. & Valenzuela, M. A. Catalyst screening for oxidative desulfurization using hydrogen peroxide. *Catal. Today*. **106**, 219–221 (2005).
11. Zhu, X. et al. Thioxanthrone-based ionic liquid as efficient and recyclable photocatalyst for α-cyanidation reaction of aromatic tertiary amines. *J. Catal.* **436**, 115605 (2024).
12. de Jesus, S. S. & Maciel Filho, R. Are ionic liquids eco-friendly? *Renew Sustain. Energy Rev* **157**(18), 112039 (2022).
13. Wang, Q., Lei, L., Zhu, J., Yang, B. & Li, Z. Deep desulfurization of fuels by extraction with 4-dimethylaminopyridinium- based ionic liquids. *Energy Fuels*. **27**, 4617–4623 (2013).
14. Mohammed, H. A., Mostafa, H. Y., El-Aty, D. M. A. & Ashmawy, A. M. Novel gemini ionic liquid for oxidative desulfurization of gas oil. *Sci. Rep.* **13**, 1–13 (2023).
15. Armandsefat, F., Hamzehzadeh, S. & Azizi, N. Efficient and promising oxidative desulfurization of fuel using Fenton like deep eutectic solvent. *Sci. Rep.* **14**, 1–13 (2024).
16. Zhang, C., Pan, X., Wang, F. & Liu, X. Extraction-oxidation desulfurization bypyridinium-based task-specific ionic liquids. *Fuel* **102**, 580–584 (2012).
17. Zhang, Z. et al. Efficient synthesis of Cyclic carbonates under atmospheric CO2 by DMAP-based ionic liquids: the difference of inert hydrogen atom and active hydrogen atom in cation. *Green. Chem. Eng.* **4**, 285–293 (2023).
18. Jiang, Y. et al. Four tartaric acid-bridged tetra-europium(III)-containing antimonotungstate with catalytic oxidation of thioethers/alcohols. *Chin. J. Struct. Chem.* **44**, 100603 (2025).
19. Wang, P. S. et al. Structural transformation from Waugh-type to Keggin-type polyoxomolybdate-based crystalline material for photo/electrocatalysis. *Rare Met.* **43**, 2241–2250 (2024).
20. Yin, P. et al. Polyoxometalate-organic hybrid molecules as amphiphilic emulsion catalysts for deep desulfurization. *Chem. - Eur. J.* **18**, 9174–9178 (2012).
21. Zang, D. et al. Interface engineering of Mo8/Cu heterostructures toward highly selective electrochemical reduction of carbon dioxide into acetate. *Appl. Catal. B Environ.* **281**, 119426 (2021).
22. Zhang, H. et al. Latest progress in covalently modified polyoxometalates-based molecular assemblies and advanced materials. *Polyoxometalates* **1**, 9140011 (2022).
23. Hu, Q., Li, K., Chen, X., Liu, Y. & Yang, G. Polyoxometalate catalysts for the synthesis of N-heterocycles. *Polyoxometalates* **3**, 9140048 (2024).
24. Rezvani, M. A., Ghasemi, K., Ardeshiri, H. H. & Aghmasheh, M. Deep oxidative desulfurization of gas oil by iron(III)-substituted polyoxometalate immobilized on nickel(II) oxide, ((n-C4H9)4 N)4H[PW11FeO39]@NiO, as an efficient nanocatalyst. *Sci. Rep.* **13**, 1–17 (2023).
25. Dong, Y. H. et al. Tuning W = O electronic structure in h-BN supported mono-substituted keggin polyoxotungstate for oxidative desulfurization. *Polyoxometalates* **4**, 9140099 (2025).
26. Zang, D. & Wang, H. Polyoxometalate-based nanostructures for electrocatalytic and photocatalytic CO2 reduction. *Polyoxometalates* **1**, 9140006 (2022).
27. Li, J., Zhang, D., Chi, Y. & Hu, C. Catalytic application of polyoxovanadates in the selective oxidation of organic molecules. *Polyoxometalates* **1**, 9140012 (2022).
28. Leng, K., Sun, Y., Zhang, X., Yu, M. & Xu, W. Ti-modified hierarchical mordenite as highly active catalyst for oxidative desulfurization of Dibenzothiophene. *Fuel* **174**, 9–16 (2016).
29. Chen, H. et al. Construction of amphiphilic and polyoxometalate poly(ionic liquids) for enhanced oxidative desulfurization in fuel. *J. Mol. Liq.* **379**, 121650 (2023).
30. Wang, Q. et al. Direct synthesis of 2,5-diformylfuran from carbohydrates via carbonizing polyoxometalate based mesoporous poly(ionic liquid). *Catal. Today*. **319**, 57–65 (2019).
31. Wu, Q. et al. Synthesis of Surface-Active Heteropolyacid-Based ionic liquids and their catalytic performance for desulfurization of fuel oils. *ACS Omega*. **5**, 31171–31179 (2020).
32. Wang, L., Wang, H. & Wang, Y. Research of desulfurization of Dibenzothiophene with SO3H-functionalized morpholine heteropolyacid ionic liquid catalyst. *J. Mol. Struct.* **1220**, 128779 (2020).
33. Lu, S. et al. An efficient and recyclable polyoxometalate-based hybrid catalyst for heterogeneous deep oxidative desulfurization of Dibenzothiophene derivatives with oxygen. *RSC Adv.* **6**, 79520–79525 (2016).
34. Li, J., Guo, Y., Tan, J. & Hu, B. Polyoxometalate dicationic ionic liquids as catalyst for extractive coupled catalytic oxidative desulfurization. *Catalysts* **11**, 1–17 (2021).
35. Norouzi, F. & Abdolmaleki, A. Acidic pyridinium ionic liquid: an efficient bifunctional organocatalyst to synthesis carbonate from atmospheric CO2 and epoxide. *Mol. Catal.* **538**, 112988 (2023).
36. Rafiee, E. & Mirnezami, F. Keggin-structured polyoxometalate-based ionic liquid salts: thermoregulated catalysts for rapid oxidation of sulfur-based compounds using H2O2and extractive oxidation desulfurization of sulfur-containing model oil. *J. Mol. Liq.* **199**, 156–161 (2014).
37. Liu, X., Li, J., Guo, Y., Wu, J. & Hu, B. Oxidative desulfurization of fuel oil catalyzed by a carbon nitride supported phosphotungstic acid based dicationic ionic liquid. *React. Chem. Eng.* **7**, 1380–1390 (2022).
38. Kashyap, N., Das, S. & Borah, R. Solvent responsive self-separation behaviour of Brønsted acidic ionic liquid-polyoxometalate hybrid catalysts on H2O2 mediated oxidation of alcohols. *Polyhedron* **196**, 114993 (2021).

39. Gao, Y., Cheng, L., Gao, R., Hu, G. & Zhao, J. Deep desulfurization of fuels using supported ionic liquid-polyoxometalate hybrid as catalyst: A comparison of different types of ionic liquids. *J. Hazard. Mater.* **401**, 123267 (2021).
40. Li, L. et al. Self-assembled vesicles containing Podophyllotoxin covalently modified with polyoxometalates for antitumor therapy. *Polyoxometalates* **4**, 1–14 (2025).
41. Dong, Y. J., Su, Z. M. & Guan, W. C(sp3)–H trifluoromethylation of pyrrolidine by [W10O32]4–/copper synergetic photocatalysis: theoretical investigation of reactivity and regioselectivity. *Polyoxometalates* **3**, 9140068 (2024).
42. Jin, D. et al. One-pot extractive and oxidative desulfurization of fuel with ternary dual-acid deep eutectic solvent. *Fuel* **329**, 125513 (2022).
43. Wang, G., Han, Y., Wang, F., Chu, Y. & Chen, X. Catalytic oxidative desulfurization of benzothiophene using silica-supported heteropolyacid catalyst: Activity, deactivation and regeneration of the catalyst. *React. Kinet Mech. Catal.* **115**, 679–690 (2015).
44. Fan, K. et al. Ternary choline chloride/benzene sulfonic acid/ethylene glycol deep eutectic solvents for oxidative desulfurization at room temperature. *RSC Adv.* **13**, 25888–25894 (2023).
45. Wang, J. et al. Engineering boron-imidazolate-based polyoxometalates for photooxidative C = C bond cleavage in aqueous media. *Polyoxometalates* **4**, 9140087 (2025).
46. Yu, Z. et al. Synthesis of carbon nitride supported amphiphilic phosphotungstic acid based ionic liquid for deep oxidative desulfurization of fuels. *J. Mol. Liq.* **308**, 113059 (2020).

Acknowledgements
We appreciate and thank the Department of Chemistry of Shiraz University for the financial support they have had in advancing this research.

Author contributions
A.A. and S.K. wrote the main manuscript text and S.K. prepared figures. All authors reviewed the manuscript.

Declarations

Competing interests
The authors declare no competing interests.

Additional information
Supplementary Information The online version contains supplementary material available at https://doi.org/10.1038/s41598-025-22466-5.

Correspondence and requests for materials should be addressed to A.A.

Reprints and permissions information is available at www.nature.com/reprints.

Publisher's note Springer Nature remains neutral with regard to jurisdictional claims in published maps and institutional affiliations.